JBC ACCELERATED COMMUNICATION

Functional analyses of a human vascular tumor FOS variant identify a novel degradation mechanism and a link to tumorigenesis

Received for publication, September 7, 2017, and in revised form, November 3, 2017 Published, Papers in Press, November 17, 2017, DOI 10.1074/jbc.C117.815845

David G. P. van IJzendoorn[‡1], Zary Forghany[§1], Frauke Liebelt[§], Alfred C. Vertegaal[§], Aart G. Jochemsen[§], Judith V. M. G. Bovée[‡], Karoly Szuhai[§2], and David A. Baker[§3]

From the Departments of [‡]Pathology and [§]Molecular Cell Biology, Leiden University Medical Center (LUMC), 2300 RC Leiden, The Netherlands

Edited by Alex Toker

Epithelioid hemangioma is a locally aggressive vascular neoplasm, found in bones and soft tissue, whose cause is currently unknown, but may involve oncogene activation. FOS is one of the earliest viral oncogenes to be characterized, and normal cellular FOS forms part of the activator protein 1 (AP-1) transcription factor complex, which plays a pivotal role in cell growth, differentiation, and survival as well as the DNA damage response. Despite this, a causal link between aberrant FOS function and naturally occurring tumors has not yet been established. Here, we describe a thorough molecular and biochemical analysis of a mutant FOS protein we identified in these vascular tumors. The mutant protein lacks a highly conserved helix consisting of the C-terminal four amino acids of FOS, which we show is indispensable for fast, ubiquitin-independent FOS degradation via the 20S proteasome. Our work reveals that FOS stimulates endothelial sprouting and that perturbation of normal FOS degradation could account for the abnormal vessel growth typical of epithelioid hemangioma. To the best of our knowledge, this is the first functional characterization of mutant FOS proteins found in tumors.

Epithelioid hemangioma is a neoplasm composed of cells that are phenotypically endothelial, which form vascular lumina or grow as solid sheets (see Fig. 1*A*) (1). Until now, the molecular underpinnings of this disease have yet to be deciphered. A recent cytogenetic and karyotypic survey of the disease, by us (2) and others (3), aimed at refining diagnoses and tumor classification, unearthed a significant number of FOS translocations raising the possibility that disruption of FOS function could promote tumorigenesis. The immediate-early *FOS* proto-oncogene is activated rapidly and transiently in response to a wide spectrum of cell stimuli (4–6), including serum, growth factors, cytokines, tumor-promoting agents, and DNA damage (7). The encoded FOS protein is a component of the crucial AP-1 transcription factor complex whose normal activity is regulated by controlled proteasome degradation (8, 9), and corruption of this process can lead to cell transformation (10–12). In this study, we have investigated the role of a novel mutant FOS protein we discovered in epithelioid hemangioma. We provide evidence that sustained expression of mutant FOS, due to loss of the C terminus, might drive the formation of vascular neoplasms by perturbing matrix metalloproteinase (MMP)[4] production and the Notch signaling pathway that are known to facilitate both physiological and pathological angiogenesis. Operationally, we found that the extreme C terminus of FOS renders it intrinsically susceptible to ubiquitin-independent degradation by the 20S proteasome, an essential mechanism bypassed by tumor FOS proteins. This is the first report of a module that directly mediates ubiquitin-independent proteasomal degradation (UIPD) and emphasizes the importance of UIPD in normal as well as tumor cells. Our work establishes the first demonstrable connection between mutations of FOS and the development of a naturally occurring tumor and unveils a potential, novel approach to treating epithelioid hemangioma by targeted inhibition of FOS or proteins whose expression is activated by FOS.

Results and discussion

C-terminally truncated FOS mutant is expressed in epithelioid hemangioma

To determine whether mutations that disrupt the normal function of FOS might promote tumorigenesis, we investigated the role of a novel mutant FOS protein in epithelioid hemangioma (Fig. 1*A*). Fig. 1*B* depicts schematically a FOS deletion mutant (hereafter termed FOSΔ) that resulted from a *FOS-MBNL1* translocation (2). The mutant transcript is predicted to encode a FOS isoform lacking the C-terminal 95 amino acids but including the bZIP domain. Western blot analysis of lysates prepared from patient tumor tissue revealed a truncated FOS protein of the expected size demonstrating that the mutant *FOS*

This work was supported by the Dutch Cancer Society Grant 30861 (to D. A. B.) and Netherlands Organization for Scientific Research Grant ZON-MW VICI 016.VICI.170.055 (to J. V. M. G. B.). The authors declare that they have no conflicts of interest with the contents of this article.

This article contains Figs. S1–S5.

The nucleotide sequence(s) reported in this paper has been submitted to the GenBank™/EBI Data Bank with accession number(s) PRJNA390521.

[1] Both authors contributed equally to this work.

[2] To whom correspondence may be addressed. E-mail: K.Szuhai@lumc.nl.

[3] To whom correspondence may be addressed. E-mail: d.baker@lumc.nl.

[4] The abbreviations used are: MMP, matrix metalloproteinase; UIPD, ubiquitin-independent proteasomal degradation; HUVEC, human umbilical vein endothelial cell; IDR, intrinsically disordered region; suc, succinyl; AMC, amido-4-methylcoumarin; qPCR, quantitative PCR; TAD, transactivation domain.

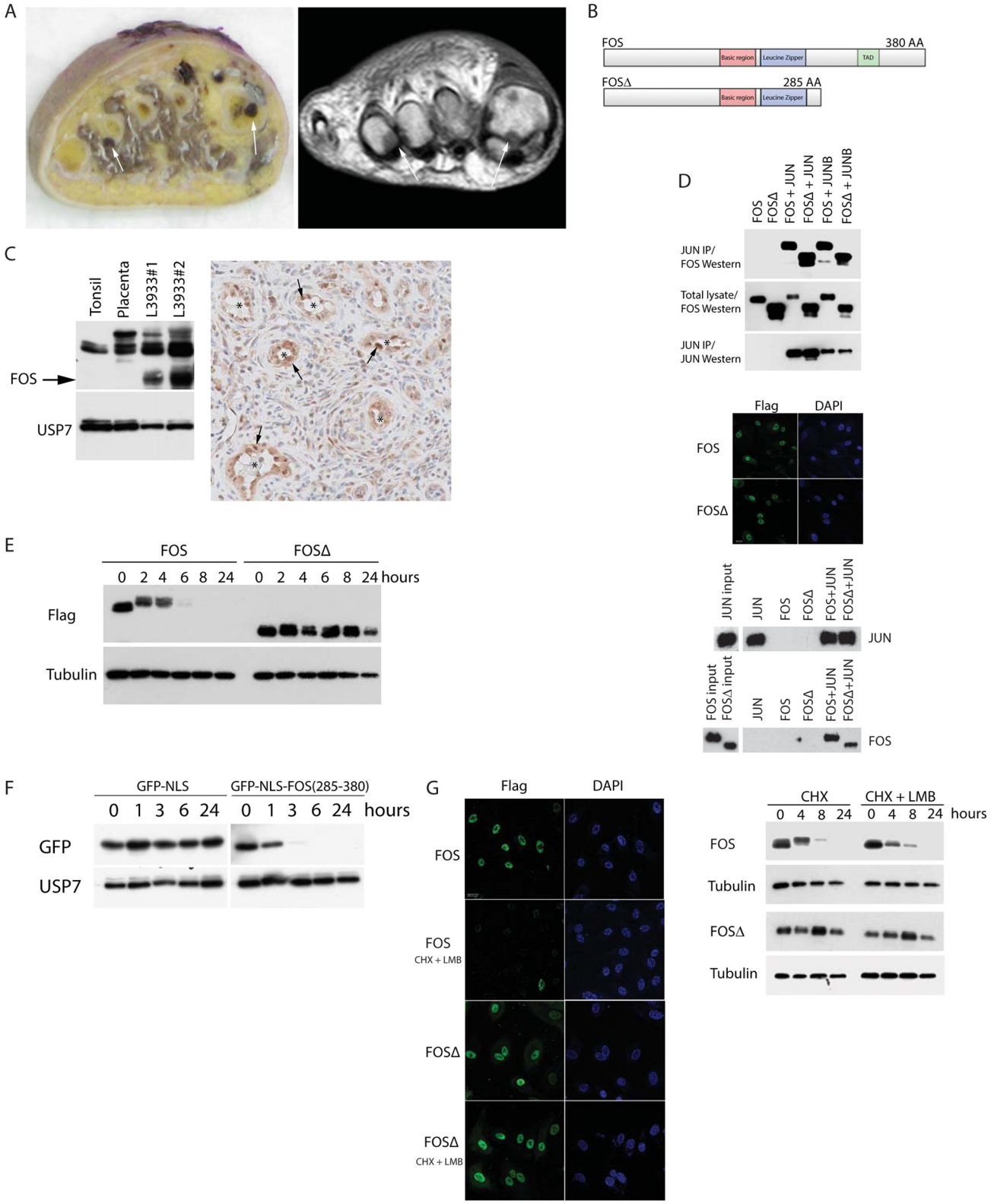

Figure 1. *A,* epithelioid hemangioma case L3933. *Left panel,* gross specimen with polyostotic localization of a hemorrhagic tumor in the 1st and 4th metatarsal bones of the foot (*arrows*). *Right panel*, corresponding T1 weighted MR image. *B,* tumor FOSΔ lacks the C-terminal 95 amino acids (including the C-terminal TAD). *IP,* immunoprecipitation. *C, left panel,* Western blot of endogenous FOS proteins in control tonsil and placenta cell lysates compared with epithelioid hemangioma tumor cell lysates. Mutant FOSΔ protein is highlighted with an *arrow*. *Right panel,* high FOS expression (*arrows*) is indicated in the endothelial cells of epithelioid hemangioma tumor blood vessels (*). *D,* AP-1 heterodimers were immunopurified from cells transfected with the indicated constructs (*top panel*). Immunofluorescence shows both FOS and FOSΔ localize to the nucleus (*middle panel*). FOS (and FOSΔ), JUN heterodimers bind to consensus AP-1 DNA-binding sites (*bottom panel*). *E,* FOS stability assay on HUVECs stably expressing FOS or FOSΔ. *F,* protein stability assay on HUVECs stably expressing either GFP or a GFP-FOS fusion (encompassing the C-terminal 95 amino acids of FOS). *G,* HUVECs expressing the indicated proteins were incubated with or without leptomycin B (*LMB*) in the presence of cycloheximide (*CHX*). *Left panel,* immunofluorescence. *Right panel,* Western blots.

gene is translated *in vivo* (Fig. 1*C*). Moreover, immunohistochemistry of tumor sections showed a significant enrichment of FOS in tumor blood vessel endothelial cells (Fig. 1*C*). In common with wild-type FOS, FOSΔ is localized to the nucleus, can heterodimerize both with JUN and JUNB, and is efficiently associated with a consensus AP-1 DNA-binding site (Fig. 1*D*). However, FOSΔ protein levels appear to be significantly higher than wild-type FOS protein levels in patient cells (see Fig. 1*C*) suggesting that the mutant protein may be aberrantly stable. To elucidate the mechanistic consequences of this deletion, we first assessed FOS protein stability in primary endothelial cells. Fig. 1*E* shows that wild-type FOS, as expected, has a relatively short half-life of ~1–2 h. By contrast, the deleted version of FOS is highly stable (half-life in excess of 8 h) suggesting that wild-type FOS harbors a destabilizing element in its C terminus, which is absent in the patient FOSΔ protein. In support of this view, tethering the FOS C terminus to a GFP reporter construct, led to a striking destabilization of the GFP protein (Fig. 1*F*), whereas a truncated FOS C terminus did not substantially alter the stability of the GFP reporter (see Fig. 3*G*). This observation is consistent with previous reports relating to FOS stability (8, 13, 14). Additionally, blocking nuclear export had no effect either on rapid FOS degradation or the stability of FOSΔ indicating that FOS is degraded in the nucleus and that FOSΔ is resistant to this process (Fig. 1*G*). The above findings were confirmed in diploid HT1080 cell and HEK293T cells indicating that this mechanism is likely to be generic.

Mutant FOS is resistant to proteasomal degradation

To precisely delineate how FOS is degraded (and why FOSΔ is not), we monitored FOS protein degradation by the proteasome. Fig. 2*A* shows that pharmacological inhibition of the proteasome, using either the specific inhibitor epoxomicin or MG132, markedly stabilized the wild-type FOS protein such that its half-life was comparable with that of the mutant FOSΔ protein. The half-life of FOSΔ was refractory to proteasome inhibition indicating that this deletion essentially lacks the motif(s) responsible for this degradative process (Fig. 2*A*). It is established that degradation by the proteasome is either ubiquitin-dependent (15) or ubiquitin-independent (16–18), and multiple different mechanisms have been reported to regulate FOS stability (19–23). In agreement with others (17, 18, 20), Fig. 2*B* shows that wild-type FOS can be ubiquitinated and subsequently processed by the 26S proteasome (see also Fig. 3*C*). We found that patient FOSΔ protein was not detectably ubiquitinated (Figs. 2*B* and 3*C*), and it fails to bind the E3 ligase, KDM2b, which has been demonstrated to stimulate FOS ubiquitination (see Fig. S1) (20). These observations could suggest that patient FOSΔ stabilization results from the absence of FOSΔ ubiquitin-dependent degradation. However, several lines of evidence support the view that the tumor FOSΔ protein is intrinsically resistant to ubiquitin-independent proteasome degradation and that this is the principal cause of its substantially increased stability. First, pharmacological inhibition of ubiquitin-activating enzymes ablated FOS ubiquitination but had no detectable impact on FOS degradation (Fig. 2*C*). In the same experiment, ubiquitin-dependent degradation of an established substrate of the proteasome, MDM2, was completely abrogated (see Fig. 2*C*). Second, wild-type non-ubiquitinated FOS but strikingly not FOSΔ was efficiently degraded by the 20S proteasome in a cell-free *in vitro* system (Fig. 2*D*). By contrast, FOS was completely resistant to degradation by the 26S proteasome under identical conditions (Fig. 2*E*). Consistent with these findings, selective inhibition of the 26S proteasome, but not the 20S proteasome (through shRNA-mediated abolition of the 19S subunits PSMD2 and PSMD14), stabilized the ubiquitinated fraction of FOS but failed to conspicuously inhibit FOS protein degradation, in sharp contrast to inhibiting both the 20S and 26S proteasomes (see Fig. 2*A*), indicating that degradation is principally via the 20S and not the 26S proteasome (Fig. S2). These results show that the FOS C terminus is vital for both ubiquitin-independent and ubiquitin-dependent proteasomal degradation and that both of these processes are lost by the mutant FOSΔ protein expressed in epithelioid hemangioma. These data show that the normal process of FOS degradation is severely corrupted in the tumor FOSΔ mutant protein and substantiate previous studies (21, 22) which suggest that FOS stability is governed chiefly by ubiquitin-independent proteasome degradation.

Mutant FOS lacks a conserved motif essential for ubiquitin-independent degradation by the 20S proteasome

To identify the motif(s) in the C terminus of FOS, which mediates FOS degradation (and is absent in FOSΔ), we performed a thorough mutational analysis of the FOS C terminus. Fig. 3*A* shows that deleting the C-terminal four amino acids was sufficient to strongly stabilize FOS and that lack of these amino acids might therefore cause the aberrant stability of the FOSΔ tumor protein. *Ab initio* modeling (24) of the FOS tail revealed that the C terminus is composed of an intrinsically unstructured region terminating in a helix composed of the C-terminal four amino acids (LLAL), which is conserved in all metazoans sequenced to date (Fig. 3*B*). Unlike FOSΔ, eliminating this helical region, either through point mutation or deletion, had no effect upon FOS ubiquitination (Fig. 3*C*). The same mutations did, however, efficiently block FOS degradation to the same degree as the tumor FOSΔ protein (see Fig. 3, *D* and *E*). The integrity of the four C-terminal amino acids, but not residues immediately adjacent to this motif, is absolutely required for priming FOS labileness (Fig. 3*F*). Deletions or point mutations of adjacent amino acids, which include consensus phosphorylation sites for ERK and GSK, failed to augment FOS stability. Indeed, a subset of these, in agreement with others (25), served to enhance FOS instability suggesting they play a role in stabilizing but not destabilizing the FOS protein (correspondingly, chemical inhibitors of MEK or deletion of the consensus ERK-docking site had a comparable effect; data not shown). Three additional experiments further validated the importance of the C-terminal motif. One, deletion of the C-terminal four amino acids strongly attenuated the capacity of the FOS C terminus to destabilize GFP (Fig. 3*G*). Two, a deletion mutant lacking the intrinsically disordered region (IDR) (which is highly stable) but retaining the C-terminal four amino acids was as unstable as wild-type FOS (Fig. 3*H*). Three, in common with tumor FOSΔ, a mutant FOS lacking the C-terminal four amino acids, was highly resistant to 20S proteasomal degradation in a cell-

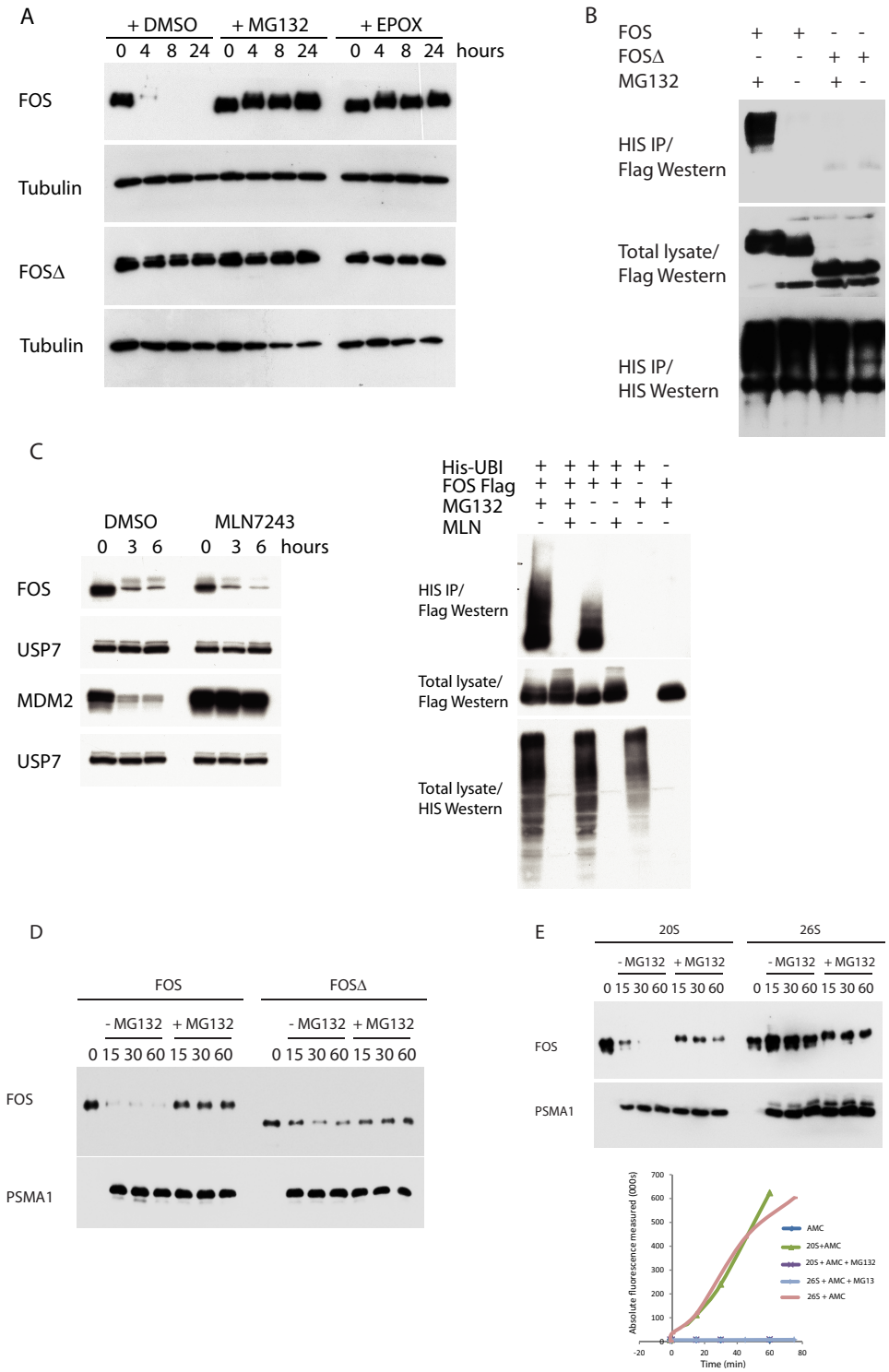

Figure 2. *A,* FOS stability assay on HUVECs stably expressing FOS or FOSΔ. *B,* ubiquitin assay of cells transfected with the indicated constructs together with 10× HIS epitope-tagged ubiquitin. *C, left panel,* FOS stability assay on HUVECs stably expressing FOS in the presence or absence of MLN7243. *Right panel,* ubiquitin assay of cells transfected with the indicated constructs and cultured in the presence or absence of MG132 and MLN7243. *IP,* immunoprecipitation. *D, in vitro* translated FOS proteins were incubated with purified 20S proteasomes for the shown time course (minutes). 20S protein levels were determined by Western blotting using an antibody directed against PSMA1. 20S proteasome activity was independently quantified using the suc-Leu-Leu-Val-Tyr-AMC peptide (as shown in *E*). *E,* experiment performed as in *D*.

free *in vitro* assay (Fig. 3*I*). These data highlight a short helical region at the extreme C terminus of FOS as a crucial determinant of FOS stability and that perturbation of this motif leads to pronounced FOS stabilization. A block in ubiquitin-independent degradation, due to loss of the extreme C terminus, is sufficient to explain mutant FOSΔ stability. Experiments in cell-free systems indicate that this motif can orchestrate direct proteasomal degradation of FOS independently of accessory proteins. IDRs have been reported to strongly influence proteasomal degradation (26), including the IDR found in the C ter-

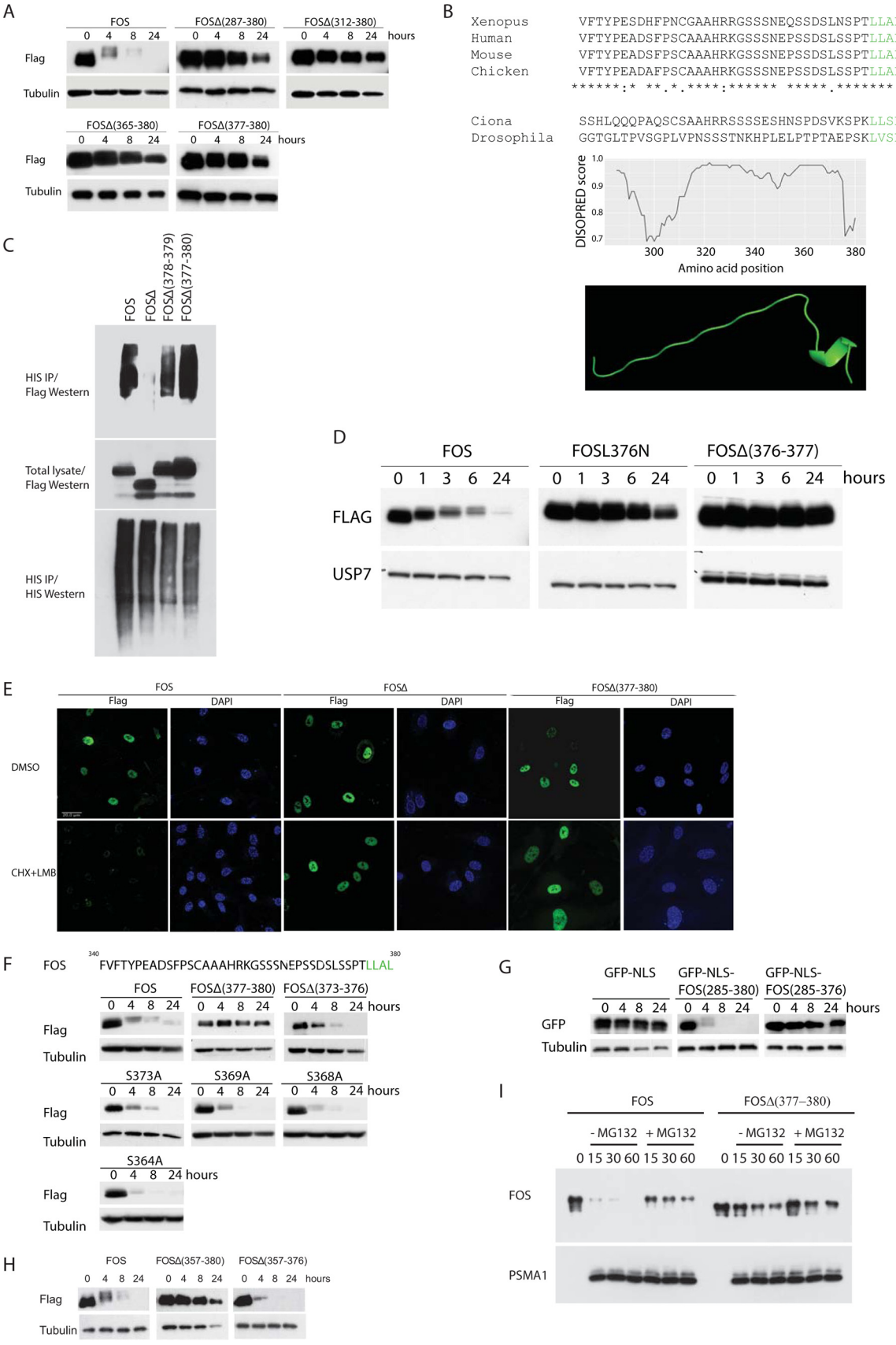
A
FOS
FOSΔ(287-380)
FOSΔ(312-380)
0 4 8 24 hours
Flag
Tubulin
FOSΔ(365-380)
FOSΔ(377-380)
B
Xenopus VFTYPESDHFPNCGAAHRRGSSSNEQSSDSLNSPTLLAL
Human VFTYPEADSFPSCAAAHRKGSSSNEPSSDSLSSPTLLAL
Mouse VFTYPEADSFPSCAAAHRKGSSSNEPSSDSLSSPTLLAL
Chicken VFTYPEADAFPSCAAAHRKGSSSNEPSSDSLSSPTLLAL
Ciona SSHLQQQPAQSCSAAHRRSSSSESHNSPDSVKSPKLLSL
Drosophila GGTGLTPVSGPLVPNSSSTNKHPLELPTPTAEPSKLVSL
DISOPRED score
Amino acid position
C
FOS
FOSΔ
FOSΔ(378-379)
FOSΔ(377-380)
HIS IP/ Flag Western
Total lysate/ Flag Western
HIS IP/ HIS Western
D
FOS
FOSL376N
FOSΔ(376-377)
0 1 3 6 24 hours
FLAG
USP7
E
FOS
FOSΔ
FOSΔ(377-380)
Flag
DAPI
DMSO
CHX+LMB
F
FOS 340 FVFTYPEADSFPSCAAAHRKGSSSNEPSSDSLSSPTLLAL 380
FOS
FOSΔ(377-380)
FOSΔ(373-376)
0 4 8 24 hours
Flag
Tubulin
S373A
S369A
S368A
S364A
G
GFP-NLS
GFP-NLS-FOS(285-380)
GFP-NLS-FOS(285-376)
0 4 8 24 hours
GFP
Tubulin
H
FOS
FOSΔ(357-380)
FOSΔ(357-376)
0 4 8 24 hours
Flag
Tubulin
I
FOS
FOSΔ(377–380)
- MG132 + MG132
0 15 30 60 15 30 60
FOS
PSMA1

minus of FOS (27). Our data show that the FOS IDR, by itself, does not stimulate FOS degradation. Rather, a highly conserved helical motif at the extreme C terminus of FOS is essential for triggering ubiquitin-independent degradation.

FOS potently stimulates endothelial sprouting

Vascular neoplasms result from the dysregulated growth of endothelial cells or their precursors (1) and represent a unique model for gaining insights into pathological as well as normal angiogenesis. To recapitulate the cell biological consequences of the mutant FOS stabilization observed in epithelioid hemangioma, we ectopically expressed wild-type and mutant FOS proteins in primary HUVECs and assessed their ability to sprout. Fig. 4*A* shows that whereas loss of FOS abolished sprouting, sustained expression of FOS strongly promoted endothelial sprouting and the formation of stable endothelial cell networks. Similarly, expression of tumor FOSΔ or FOS lacking an intact C-terminal four amino acids strongly stimulated endothelial sprouting of HUVECs (Fig. 4*B*). This phenomenon was independent of marked changes in cell proliferation (Fig. 4*B*). Fig. S3 shows that FOS and FOSΔ also stimulated sprouting of human lung microvascular endothelial cells. The endothelial cell networks produced by cells expressing FOS and FOSΔ were stable and persistent. In this assay, ordinarily the sprouting network is relatively short-lived and collapses after ~24 h. By contrast, endothelial cell networks expressing elevated levels of FOS and FOSΔ were sustained for at least 2 weeks of culture (sprouting networks expressing FOSΔ were noticeably more robust than the wild-type FOS-expressing networks), which resembles the illicit vessel growth observed in human epithelioid hemangioma.

Mutant FOS-driven sprouting is dependent on MMPs and Notch signaling

To understand the mechanistic basis of FOS-driven sprouting, we performed global transcriptome analyses of sprouts formed by FOS or patient FOSΔ-expressing primary endothelial cells. Fig. 4*C* shows a confirmatory qPCR of a selection of angiogenesis-control genes, which were up-regulated, including MMPs and components of the Notch-signaling pathway that are known to facilitate both physiological and pathological angiogenesis (28–33). ChIP analyses showed that endogenous FOS bound to these promoters (Fig. S4), and complementary ChIP studies showed that FOSΔ directly interacts with these promoters (see Fig. 4*C*). Our experiments uncover a previously unreported role for FOS as an activator of endothelial sprouting and show that patient FOSΔ could stimulate illicit endothelial sprouting by activating the Notch signaling pathway and increasing the production of MMPs. In this regard, it is notable that inhibitors of either MMPs or Notch signaling significantly inhibited the sprouting of FOSΔ-expressing endothelial cells (Fig. 4*D*). The same inhibitors had relatively little effect on cells expressing wild-type FOS under these assay conditions. This could reflect the fact that both MMP production and Notch signaling (as well as other FOS target pathways, see under "Transcriptome profiling) were significantly more augmented in cells expressing wild-type FOS compared with cells expressing FOSΔ (presumably because FOSΔ lacks the C-terminal TAD). Accordingly, a recently reported small molecule inhibitor of FOS (34), which has advanced to human Phase II clinical trials for the treatment of rheumatoid arthritis, efficiently inhibited FOS-driven endothelial sprouting (Fig. S5).

In summary, our data have uncovered a previously unreported role for FOS in stimulating endothelial cell sprouting. We show that sustained expression of FOS, due to loss of the C terminus, could drive the formation of vascular neoplasms. By analyzing the C-terminal region of FOS, which is deleted in epithelioid hemangioma, we have discovered a highly conserved motif at the extreme C terminus of FOS that is critical for controlling its stability by rendering it intrinsically susceptible to ubiquitin-independent degradation by the 20S proteasome. Our work suggests that targeted inhibition of FOS or proteins whose expression is activated by FOS might represent a legitimate novel approach to treating these locally aggressive tumors.

Experimental procedures

Patient samples

Epithelioid hemangioma case L3933 was acquired from the archives of the Leiden University Medical Center (LUMC), Leiden, The Netherlands. The diagnosis of epithelioid hemangioma was established by a bone and soft tissue pathologist (J. V. M. G. B.). The study was approved by the LUMC Medical Ethical Commission under protocol B17006.

Cell culture, biochemistry, and molecular biology

Primary HUVECs (Lonza) were cultured in EGM2 medium (Lonza). Chondrosarcoma HT1080 and human embryonic kidney 293T cells were cultured in DMEM (Gibco) supplemented with 10% fetal bovine serum (Gibco). Transfections, lentivirus production and cell infections, Western blotting, and co-immunoprecipitations have been described previously (35). FOS stability assays were performed by incubating cells in the presence or absence of cycloheximide for a defined time course (hours). Protein levels were determined by Western blotting.

Plasmid and shRNA construction

Human *FOS* cDNAs fused in-frame with a FLAG or an HA epitope tag were cloned into the pLV lentiviral vector and pCS2

Figure 3. *A,* FOS stability assay on HUVECs stably expressing the indicated FOS deletion mutants. *B, ab initio* modeling of the FOS C terminus. *C,* ubiquitin assay performed on cells transfected with the indicated constructs together with 10× HIS epitope-tagged ubiquitin. Cells were cultured in the presence of MG132. *IP,* immunoprecipitation. *D,* FOS stability assay on HUVECs stably expressing the indicated FOS deletion mutants. *E,* HUVECs expressing the indicated proteins were incubated with or without leptomycin B (*LMB*) in the presence of cycloheximide (*CHX*). FOS was visualized by immunofluorescence. *F,* FOS stability assay on HUVECs stably expressing the indicated FOS deletion mutants. *G,* protein stability assay on HUVECs stably expressing either GFP, a GFP-FOS fusion (encompassing the C-terminal 95 amino acids of FOS), or the same fusion lacking the last four amino acids of FOS. *H,* FOS stability assay on HUVECs stably expressing the indicated FOS deletion mutants. FOSΔ(357–380) lacks the C-terminal 23 amino acids (the IDR). FOSΔ(357–376) lacks the IDR but retains the C-terminal four amino acids. *I, in vitro* FOS stability assay as described in Fig. 2, *D* and *E*.

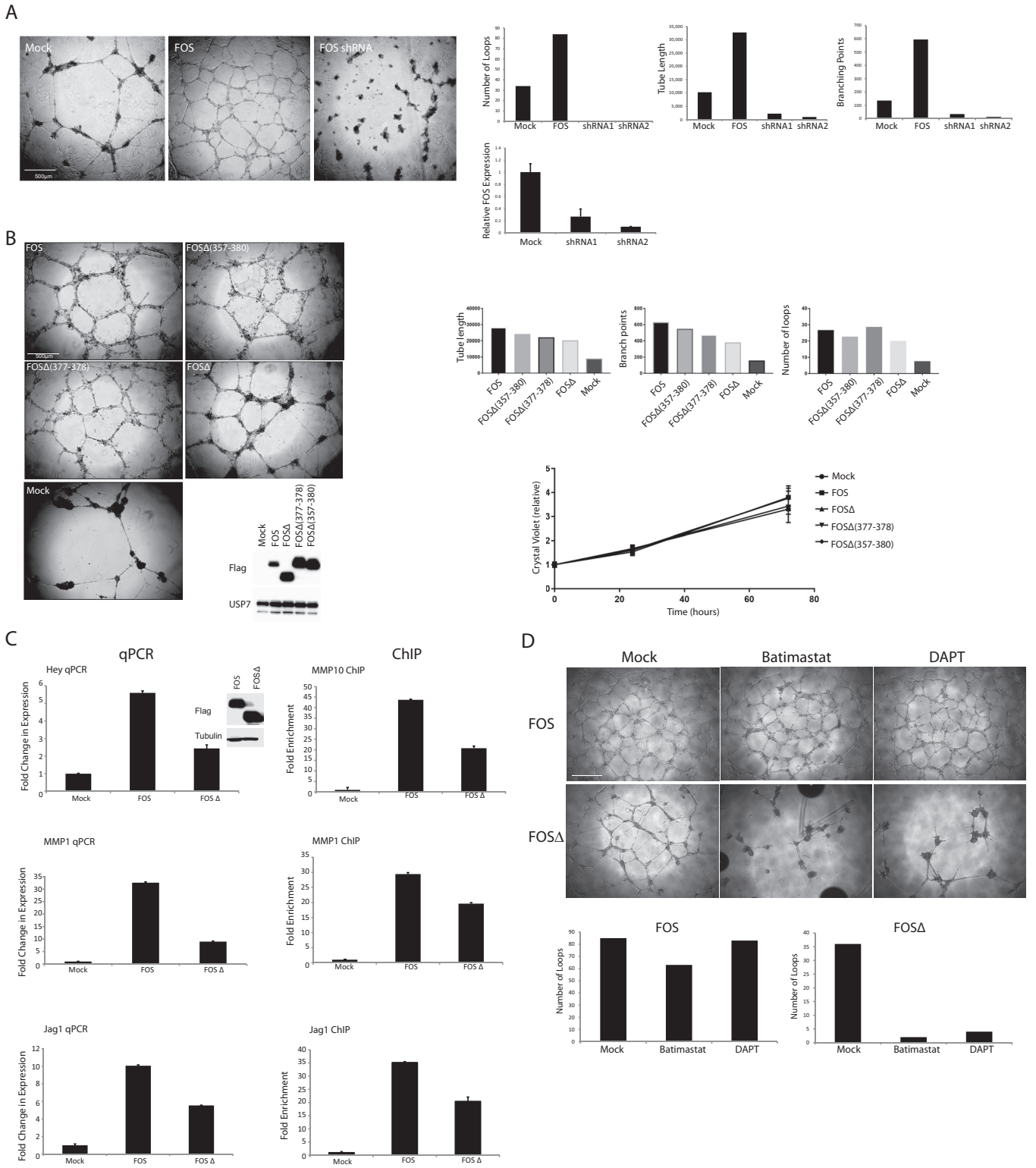

Figure 4. *A,* HUVECs lacking endogenous FOS or ectopically expressing wild-type FOS were grown on Matrigel. A representative of several independent experiments is shown. Sprouting was quantified after 24 h using in-house computer software. Loss of *FOS* was determined by qPCR (*lowermost graph*). *B,* Matrigel sprouting assay (see *A*) on HUVECs stably expressing the indicated FOS proteins. *Lower graph,* cell proliferation assay of the same HUVECs lines. Triplicate measurements were made at each time point. Values are means ± S.E. of the mean. *C, left panel,* expression levels of the indicated transcripts in HUVECs were determined by real-time qPCR. All values were averaged relative to TATA-binding protein (*TBP*), signal recognition particle receptor (*SRPR*), and calcium-activated neutral proteinase 1 (*CAPNS1*). Values were normalized against mock-treated cells. Values represent ± S.D. ($n = 3$). *Right panel,* a ChIP analysis of FOS association with the indicated promoters in HUVECs stably expressing FOS or tumor FOSΔ. Three different primer sets were used for each promoter region. A single representative is shown (all three gave similar results). Results are presented as mean fold changes in recovery (as a fraction of input) relative to the Mock infected cells. *Error bars* represent the standard deviation ($n = 3$). Relative FOS and FOSΔ protein levels were determined by Western blotting. *D,* HUVECs stably expressing the indicated FOS proteins were grown on Matrigel in the presence or absence of the MMP inhibitor, batimastat (10 μM), or the γ-secretase inhibitor, DAPT (10 μM). Sprouting was quantified after 48 h.

expression plasmid. Gene-specific shRNA-expressing lentiviruses were generated using the TRC2-pLKO lentiviral vector system.

Transcriptome profiling

RNA was isolated from HUVECs stably expressing FOS or FOSΔ by treatment with TRIzol (Invitrogen) column purification (Direct-zol RNA isolation kit-Zymo Research). RNA quality was verified with a Bioanalyzer (Agilent), and sequencing was performed on the Illumina HiSeq 2500 (Genome Scan). HUVEC transcript sequencing data have been deposited under GenBank™ accession no. PRJNA390521.

Analysis of mRNA expression

RNA isolation, first strand cDNA synthesis, and analysis of expression of transcripts by quantitative PCR were performed as described previously (33).

Ubiquitination assay

293T cells were transfected with the appropriate plasmids. Proteasome degradation was blocked for 8 h with 10 μM MG132 (Sigma). HIS pulldowns were performed as described previously (36).

HUVEC sprouting assay

96-well plates were coated with 60 μl of Matrigel/well 30 min prior to seeding HUVECs. EGM-2 medium was supplemented with 50 ng/ml recombinant human VEGF 165 (R & D Systems). Images were taken at multiple time points. Analysis of the sprouting was performed with Stacks (in-house software, Department of Molecular Cell Biology, LUMC).

Immunohistochemistry/Immunofluorescence

Staining was performed on 4-μm tissue sections. Paraffin was removed with xylene, and sections were rehydrated in a gradient of ethanol. Exogenous peroxidase was blocked using 0.3% H_2O_2. Microwave antigen retrieval was performed in Tris-EDTA (pH 9.0). FOS antibody was used at a 1:400 concentration. Antibody was detected with 3,3′-diaminobenzidine, and counterstaining was performed with hematoxylin. Immunostaining was performed as described previously (37).

Proteasome purification and in vitro degradation assay

HT1080 cells, stably expressing GFP-PSMD12, were lysed in buffer containing 40 mM Tris (pH 7.5), 40 mM NaCl, 2 mM β-mercaptoethanol, 5 mM $MgCl_2$, 2 mM ATP, 10% glycerol, and 0.5% Nonidet P-40. Lysates were cleared by ultracentrifugation at 36,000 rpm for 45 min at 4 °C. Cleared lysates were incubated for 3 h at 4 °C with prewashed Chromotek GFP-Trap® bead slurry. Beads were washed four times in wash buffer containing 40 mM Tris (pH 7.5), 40 mM NaCl, 2 mM β-mercaptoethanol, 5 mM $MgCl_2$, 2 mM ATP, and 10% glycerol. Activity of purified 26S proteasome and 20S proteasome (Enzo LifeSciences) was measured using 100 μM suc-LLVY-AMC substrate (Bachem) in a buffer containing 50 mM Tris (pH 7.5), 40 mM KCl, 5 mM $MgCl_2$, 1 mM DTT (0.5 mM ATP for the 26S proteasome) (absorbance/emission = 353/442 nm). *In vitro*-translated FOS proteins were prepared using the TNT-coupled reticulocyte *in vitro* translation system (Promega). Cell-free degradation assays were performed as described previously (38).

Protein–DNA interaction assays

In vitro-translated protein was made as above. 50 pmol of biotinylated double-stranded oligonucleotides harboring three contiguous AP-1 DNA-binding sites were coupled to MyOne streptavidin C1 beads (Invitrogen). Reactions were incubated at 4 °C with vigorous shaking for 30 min in the presence of 1 μg of poly(dI/dC), 4 mM spermidine, 50 mM KCl, 10 mM HEPES (pH 7.6), 5 mM $MgCl_2$, 10 mM Tris (pH 8), 0.05 mM EDTA (pH 8), 0.1% Triton X-100, and 20% glycerol. Beads were successively washed three times with the aforementioned buffer. Associated proteins were eluted in Laemmli buffer, and protein–DNA interactions were determined by Western blotting.

ChIP

ChIP analyses were performed on confluent 10-cm tissue culture dishes of HUVECs as described previously (35).

Antibodies, growth factor, and drugs

Antibodies were obtained from the following sources: FLAG mouse M2 monoclonal (Sigma); anti-HA.11 mouse monoclonal (Covance); anti-FOS rabbit (Cell Signaling); anti-HA rabbit polyclonal (Abcam); anti-FOS rabbit (Sigma); anti-FLAG rabbit (Sigma); anti-USP7 rabbit (Bethyl); anti-γ-tubulin (Sigma); anti-GFP (GeneTex); anti-His (Sigma); and anti-PSMA1 (Sigma). Drugs were used at the following concentrations: MG132 (Sigma), 10 μM; cycloheximide (Sigma), 50 μg/ml; epoxomicin (Sigma), 10 μM; leptomycin B (Sigma) 35 nM; MLN-7243 (Active Biochem), 10 μM; Batimastat (Calbiochem), 10 μM; DAPT (Tocris Bioscience), 10 μM.

Bioinformatics

Rosetta (RosettaCommons) was used for structure prediction of the FOS C terminus (24). Secondary structure was predicted using Psipred (version 4.01, UCL). Degree of disorder was predicted using Disopred (version 3.16, UCL).

Author contributions—Z. F. and D. G. P v. I. performed the majority of experiments. F. L. and A. C. V. helped design and performed *in vitro* proteasome studies. J. V. M. G. B. and A. G. J. offered expert advice. K. S. and D. A. B. supervised the study. All authors read and approved the paper.

Acknowledgments—We thank members of the Departments of Molecular Cell Biology and Pathology for helpful discussions, technical advice, and support especially from Hans van Dam and Professor Peter ten Dijke. We acknowledge Inge Briaire-de Bruijn for technical assistance with the immunohistochemistry. We are indebted to Dr. Hans Vrolijk for designing computer software for quantifying sprouting assays.

References

1. Rosenberg, A. E., and Bovée, J. V. (2013) in *WHO Classification of Tumours of Soft Tissue and Bone* (Fletcher, C. D., Bridge, J. A., Hogendoorn, P. C., and Mertens, F., eds) pp. 333–334, IARC Press, Lyon, France
2. van IJzendoorn, D. G., de Jong, D., Romagosa, C., Picci, P., Benassi, M. S., Gambarotti, M., Daugaard, S., van de Sande, M., Szuhai, K., and Bovée,

J. V. (2015) Fusion events lead to truncation of FOS in epithelioid hemangioma of bone. *Genes Chromosomes Cancer* **54,** 565–574
3. Huang, S. C., Zhang, L., Sung, Y. S., Chen, C. L., Krausz, T., Dickson, B. C., Kao, Y. C., Agaram, N. P., Fletcher, C. D., and Antonescu, C. R. (2015) Frequent FOS gene rearrangements in epithelioid hemangioma: A molecular study of 58 cases with morphological reappraisal. *Am. J. Surg. Pathol.* **39,** 1313–1321
4. Wagner, E. F. (2001) AP-1 reviews. *Oncogene* **20,** 2333–2497
5. Johnson, R. S., Spiegelman, B. M., and Papaioannou, V. (1992) Pleiotropic effects of a null mutation in the c-fos proto-oncogene. *Cell* **71,** 577–586
6. Shaulian, E., and Karin, M. (2002) AP-1 as a regulator of cell life and death. *Nat. Cell Biol.* **4,** E131–E136
7. Haas, S., and Kaina, B. (1995) c-Fos is involved in the cellular defence against the genotoxic effect of UV radiation. *Carcinogenesis* **16,** 985–991
8. Wilson, T., and Treisman, R. (1988) Fos C-terminal mutations block down-regulation of c-fos transcription following serum stimulation. *EMBO J.* **7,** 4193–4202
9. Gomard, T., Jariel-Encontre, I., Basbous, J., Bossis, G., Moquet-Torcy, G., Mocquet-Torcy, G., and Piechaczyk, M. (2008) Fos family protein degradation by the proteasome. *Biochem. Soc. Trans.* **36,** 858–863
10. Van Beveren, C., van Straaten, F., Curran, T., Müller, R., and Verma, I. M. (1983) Analysis of FBJ-MuSV provirus and c-fos (mouse) gene reveals that viral and cellular fos gene products have different carboxy termini. *Cell* **32,** 1241–1255
11. Eferl, R., and Wagner, E. F. (2003) AP-1: A double-edged sword in tumorigenesis. *Nat. Rev. Cancer* **3,** 859–868
12. Monje, P., Marinissen, M. J., and Gutkind, S. (2003) Phosphorylation of the carboxyl-terminal transactivation domain of c-Fos by extracellular signal-regulated kinase mediates the transcriptional activation of AP-1 and cellular transformation induced by platelet-derived growth factor. *Mol. Cell. Biol.* **23,** 7030–7043
13. Ferrara, P., Andermarcher, E., Bossis, G., Acquaviva, C., Brockly, F., Jariel-Encontre, I., and Piechaczyk, M. (2003) The structural determinants responsible for c-Fos protein proteasomal degradation differ according to the conditions of expression. *Oncogene* **22,** 1461–1474
14. Acquaviva, C., Brockly, F., Ferrara, P., Bossis, G., Salvat, C., Jariel-Encontre, I., and Piechaczyk, M. (2001) Identification of a tripeptide motif involved in the control of rapid proteasomal degradation of c-Fos proto-oncogene during the G_0-to-S phase transition. *Oncogene* **20,** 7563–7572
15. Collins, G. A., and Goldberg, A. L. (2017) The logic of the 26S proteasome. *Cell* **169,** 792–806
16. Erales, J., and Coffino, P. (2014) Ubiquitin-independent proteasomal degradation. *Biochem. Biophys. Acta* **1843,** 216–221
17. Jariel-Encontre, I., Bossis, G., and Piechaczyk, M. (2008) Ubiquitin-independent degradation of proteins by the proteasome. *Biochem. Biophys. Acta* **1786,** 153–177
18. Ben-Nissan, G., and Sharon, M. (2014) Regulating the 20S proteasome ubiquitin-independent degradation pathway. *Biomolecules* **4,** 862–884
19. Stancovski, I., Gonen, H., Orian, A., Schwartz, A. L., and Ciechanover, A. (1995) Degradation of the proto-oncogene product c-Fos by the ubiquitin proteolytic system *in vivo* and *in vitro*: identification and characterization of the conjugating enzymes. *Mol. Cell. Biol.* **15,** 7106–7116
20. Han, X.-R., Zha, Z., Yuan, H. X., Feng, X., Xia, Y. K., Lei, Q. Y., Guan, K. L., and Xiong, Y. (2016) KDM2B/FBXL10 targets c-Fos for ubiquitylation and degradation in response to mitogenic stimulation. *Oncogene* **35,** 4179-4190
21. Adler, J., *et al.* (2010) c-Fos proteasomal degradation is activated by a default mechanism and its regulation by NAD(P)H:Quinone oxidoreductase 1 determines c-Fos serum response kinetics. *Mol. Cell. Biol.* **30,** 3767–3778
22. Sasaki, T., Kojima, H., Kishimoto, R., Ikeda, A., Kunimoto, H., and Nakajima, K. (2006) Spatiotemporal regulation of c-Fos by ERK5 and the E3 ubiquitin ligase UBR1, and its biological role. *Mol. Cell* **24,** 63–75
23. Bossis, G., Ferrara, P., Acquaviva, C., Jariel-Encontre, I., and Piechaczyk, M. (2003) c-Fos proto-oncogene is degraded by the proteasome independently of its own ubiquitinylation *in vivo*. *Mol. Cell. Biol.* **23,** 7425–7436
24. Baker, D. (2014) Protein folding, structure prediction and design. *Biochem. Soc. Trans.* **42,** 225–229
25. Okazaki, K., and Sagata, N. (1995) The Mos/MAP kinase pathway stabilizes c-Fos by phosphorylation and augments its transforming activity in NIH 3T3 cells. *EMBO J.* **14,** 5048–5059
26. Prakashm S., Tian, L., Ratliff, K. S., Lehotzky, R. E., and Matouschek, A.(2004) An unstructured initiation site is required for efficient proteasome-mediated degradation. *Nat. Struct. Mol. Biol.* **11,** 830–837
27. Campbell, K. M., Terrell, A. R., Laybourn, P. J., and Lumb, K. J. (2000) Intrinsic structural disorder of the C-terminal activation domain from the bZIP transcription factor Fos. *Biochemistry* **39,** 2708–2713
28. Heo, S.-H., Choi, Y. J., Ryoo, H. M., and Cho, J. Y. (2010) Expression profiling of ETS and MMP factors in VEGF-activated endothelial cells: Role of MMP-10 in VEGF induced angiogenesis. *J. Cell. Physiol.* **224,** 734–742
29. Lee, S., Jilani, S. M., Nikolova, G. V., Carpizo, D., and Iruela-Arispe, M. L. (2005) Processing of VEGF-A by matrix metalloproteinases regulates bioavailability and vascular patterning in tumors. *Cell Biol. J.* **169,** 681–691
30. Juncker-Jensen, A., Deryugina, E. I., Rimann, I., Zajac, E., Kupriyanova, T. A., Engelholm, L. H., and Quigley, J. P (2013) Tumor MMP-1 activates endothelial PAR1 to facilitate vascular intravasation and metastatic dissemination. *Cancer Res.* **73,** 4196–4211
31. Kopan, R., and Ilagan, M. X. (2009) The canonical Notch signaling pathway: unfolding the activation. *Cell* **137,** 216–233
32. Herbert, S. P., and Stainier, D. Y. (2011) Molecular control of endothelial cell behavior during blood vessel morphogenesis. *Nat. Rev. Mol. Cell Biol.* **12,** 551–564
33. Adams, R. H., and Alitalo, K. (2007) Molecular regulation of angiogenesis and lymphangiogenesis. *Nat. Rev. Mol. Cell Biol.* **8,** 464–478
34. Ye, N., Ding, Y., Wild, C., Shen, Q., and Zhou, J. (2014) Small molecule inhibitors targeting activator protein 1 (AP-1). *J. Med. Chem.* **57,** 6930–6948
35. Roukens, M. G., Alloul-Ramdhani, M., Baan, B., Kobayashi, K., Peterson-Maduro, J., van Dam, H., Schulte-Merker, S., and Baker, D. A. (2010) Control of endothelial sprouting by a Tel-CtBP complex. *Nat. Cell Biol.* **12,** 933–942
36. Roukens, M. G., Alloul-Ramdhani, M., Moghadasi, S., Op den Brouw, M., and Baker, D. A. (2008) Downregulation of vertebrate Tel (ETV6) and *Drosophila* Yan is facilitated by an evolutionarily conserved mechanism of F-box-mediated ubiquitination. *Mol. Cell. Biol.* **28,** 4394–4406
37. Roukens, M. G., Alloul-Ramdhani, M., Vertegaal, A. C., Anvarian ,Z., Balog, C. I., Deelder, A. M., Hensbergen, P. J., and Baker, D. A. (2008) Identification of a new site of sumoylation on Tel (ETV6) uncovers a PIAS-dependent mode of regulating Tel function. *Mol. Cell. Biol.* **28,** 2342–2357
38. Asher, G., Tsvetkov, P., Kahana, C., and Shaul, Y. (2005) A mechanism of ubiquitin-independent proteasomal degradation of the tumor suppressors p53 and p73. *Genes Dev.* **19,** 316–321